Magnetic Properties of Lone-Pair-Containing, Sandwich-Type Polyoxoanions: A Detailed Study of the Heteroatomic Effect

Ashley C. Stowe,[a] Saritha Nellutla,[a] Naresh S. Dalal,*[a] and Ulrich Kortz*[b]

Keywords: Copper / EPR spectroscopy / Magnetic properties / Polyoxometalates / Self assembly / Tungsten

Magnetic susceptibility and high-frequency EPR spectroscopy investigations were carried out on the isostructural family of tricopper(II)-substituted, sandwich-type polyoxotungstates $[Cu_3(H_2O)_3(\alpha\text{-}AsW_9O_{33})_2]^{12-}$ (**1**), $[Cu_3(H_2O)_3(\alpha\text{-}SbW_9O_{33})_2]^{12-}$ (**2**), $[Cu_3(H_2O)_3(\alpha\text{-}SeW_9O_{33})_2]^{10-}$ (**3**), and $[Cu_3(H_2O)_3(\alpha\text{-}TeW_9O_{33})_2]^{10-}$ (**4**) with the intention of examining the possible influence of the diamagnetic heteroatoms X (X = As^{III}, Sb^{III}, Se^{IV}, Te^{IV}) on the magnetic exchange properties of the three Cu^{2+} ions in the central belt. Magnetic susceptibility data indicate a single antiferromagnetic spin exchange constant J for the triangular Cu_3 belts in **1**–**4**. Variable-temperature, W-band (ca. 94 GHz) EPR spectra reveal that the Cu_3 units have $S_T = 1/2$ as the spin ground state with the excited state $S_T = 3/2$ located within a few cm^{-1}. We also determined the g matrix components for both the $S_T = 1/2$ and 3/2 states. The zero-field parameter D has been measured for the $S_T = 3/2$ state, and its sign is shown to be positive for **1**–**4**. From the analysis of the g matrix components for the molecular and the local Cu^{2+} site symmetry, the unpaired electrons are shown to occupy the $3d_{x^2-y^2}$ orbitals. The J values change from –1.36 to –1.04 cm^{-1} for **1** and **2**, and from –1.52 to –1.48 cm^{-1} for **3** and **4**, respectively. The g values follow a similar trend, but the D value for **4** implies a role of through-space as well as through-bond sources for the magnetic interactions in the Cu_3 belt. Our results suggest that the heteroatoms, containing lone pairs, allow the fine tuning of the magnetic parameters of **1**–**4**.

Introduction

Polyoxoanions constitute a rapidly growing class of molecular metal−oxygen clusters with an enormous diversity of structures.[1,2] These molecules also display a unique multitude of properties based on their highly alterable sizes, shapes, charge densities, and reversible redox potentials. As a consequence, possible applications span a wide range of domains including catalysis, electrocatalysis, medicine, materials science, photochemistry, analytical chemistry and magnetochemistry.[3−6]

The synthesis of new classes of compounds with ground states with high electronic spin, S, is a topic of high current interest in synthetic chemistry, fundamental theoretical understanding of quantum phenomenon and future nanotechnology.[7] Incorporation of multiple transition metal ions in lacunary polyoxoanion fragments can lead to species with various stoichiometries and structural features combined with interesting magnetic properties.[8] Thus, studies of well-characterized polyoxoanions containing exchange-coupled paramagnetic metal centers should add useful data to the literature on polyoxometalates. Polyoxoanions can be considered as intermediate in complexity between monomeric metal coordination complexes and high-spin multinuclear clusters that have received considerable attention.[9−12] Since in polyoxoanions the magnetic fragment is usually encapsulated by a diamagnetic tungsten−oxo cluster, they provide ideal structural supports for the study of the magnetic exchange interactions in clusters.[13,14]

Although an enormous number of polyoxoanions with different structures is known, there are relatively few isostructural polyoxoanion families that contain several, well-characterized members. Probably the best known examples are the tetrametal-substituted, sandwich-type polyoxotungstates of the Keggin type $\{[M_4(H_2O)_2(B\text{-}\alpha\text{-}XW_9O_{34})_2]$ (M = Mn^{2+}, Fe^{3+}, Co^{2+} etc.; X = P, As, Si, Ge)$\}$ and the Wells−Dawson analogues $\{[M_4(H_2O)_2(B\text{-}\alpha\text{-}X_2W_{15}O_{34})_2]$ (M = Mn^{2+}, Fe^{3+}, Co^{2+} etc.; X = P, As)$\}$.[8b,15] Over the last decade or so the magnetic properties of transition-metal-substituted polyanions have been investigated predominantly by Coronado et al.[16] In these studies the properties of derivatives containing different transition metals (e.g. Cu^{2+} vs. Mn^{2+}) were investigated. There is essentially no report on a systematic, comparative magnetic study of isostructural polyoxoanions involving the heteroatoms.

[a] Department of Chemistry and Biochemistry, Florida State University and National High Magnetic Field Laboratory and Center for Interdisciplinary Magnetic Resonance,
Tallahassee, FL 32306-4390, USA
Fax: (internat.) + 1-850-644-3398
E-mail: dalal@chemmail.chem.fsu.edu
[b] International University Bremen, School of Engineering and Science,
P. O. Box 750561, 28725 Bremen, Germany
Fax: (internat.) + 49-421-200-3229
E-mail: u.kortz@iu-bremen.de

  DOI: 10.1002/ejic.200400234

The $(Cu^{2+})_3$ fragment represents the simplest example of a spin-frustrated system, provided (i) the exchange interaction is antiferromagnetic and (ii) the copper centers are symmetry-related through a C_3 axis. The compounds studied here belong to this class. Although many compounds containing a $(Cu^{2+})_3$ fragment have been reported, there is no system that allows one to fine-tune the magnetic interactions of the $(Cu^{2+})_3$ moiety.[17−25] Polyoxometalates appear to be an excellent candidate for such a study.

Recently Kortz et al. reported on the synthesis and structural characterization of the four copper(II)-substituted, lone-pair-containing polyoxotungstates $[Cu_3(H_2O)_3(\alpha\text{-}AsW_9O_{33})_2]^{12-}$ (**1**), $[Cu_3(H_2O)_3(\alpha\text{-}SbW_9O_{33})_2]^{12-}$ (**2**), $[Cu_3(H_2O)_3(\alpha\text{-}SeW_9O_{33})_2]^{10-}$ (**3**), and $[Cu_3(H_2O)_3(\alpha\text{-}TeW_9O_{33})_2]^{10-}$ (**4**).[26] The isostructural nature of polyanions **1**−**4** allows one to correlate the magnetic properties of these compounds with structural details.

We used high-frequency EPR spectroscopy and SQUID magnetometry to study the effects of heteroatomic substitution on the magnetic properties of **1**−**4** and we discovered an interesting trend.

Results and Discussion

For the study reported here we used $Na_{12}[Cu_3(H_2O)_3(\alpha\text{-}AsW_9O_{33})_2]\cdot 32H_2O$ (**Na-1**), $Na_{12}[Cu_3(H_2O)_3(\alpha\text{-}SbW_9O_{33})_2]\cdot 46H_2O$ (**Na-2**), $K_9Na[Cu_3(H_2O)_3(\alpha\text{-}SeW_9O_{33})_2]\cdot 16H_2O$ (**K-3**) and $K_9Na[Cu_3(H_2O)_3(\alpha\text{-}TeW_9O_{33})_2]\cdot 16H_2O$ (**K-4**) which were synthesized according to the published procedure.[26]

The copper(II)-substituted, lone-pair-containing polyoxotungstates $[Cu_3(H_2O)_3(\alpha\text{-}AsW_9O_{33})_2]^{12-}$ (**1**), $[Cu_3(H_2O)_3(\alpha\text{-}SbW_9O_{33})_2]^{12-}$ (**2**), $[Cu_3(H_2O)_3(\alpha\text{-}SeW_9O_{33})_2]^{10-}$ (**3**), and $[Cu_3(H_2O)_3(\alpha\text{-}TeW_9O_{33})_2]^{10-}$ (**4**) consist of two $(\alpha\text{-}XW_9O_{33})$ units joined by three equivalent Cu^{2+} ions (see Figure 1). All copper ions have one terminal water molecule resulting in a square-pyramidal coordination geometry. Therefore, these polyanions have idealized D_{3h} symmetry. The space in between the three transition metal ions is occupied by three sodium ions (X = As^{III}, Sb^{III}) or potassium ions (X = Se^{IV}, Te^{IV}) leading to a central belt of six metal atoms alternating in position.

The separations of the three copper ions and the two heteroatoms in polyanions **1**−**4** are summarized in Table 1.

Magnetic Susceptibility

Figure 2 shows a plot of $\chi_m T$ vs. T for compound **K-4**. This type of behavior indicates the presence of antiferromagnetic exchange interactions between the Cu^{2+} ions. The behavior of compounds **Na-1**, **Na-2** and **K-3** is very similar. The solid-state structures of polyanions **1**−**4** indicated that two of the three copper centers are crystallographically inequivalent, but nevertheless all three are oriented in a very regular triangular fashion.[26] Therefore, we used the equilateral triangle model in order to explain the observed magnetic properties of **Na-1**, **Na-2**, **K-3** and **K-4**. The Heisenberg spin exchange Hamiltonian corresponding to this model is given in Equation (1).[24,25,27] Here J is the spin exchange coupling constant, and $\hat{S}_i$ (i = 1, 2, 3) is the spin operator of the ith ion. The eigenvalues associated with the Hamiltonian in Equation (1) can be given as in

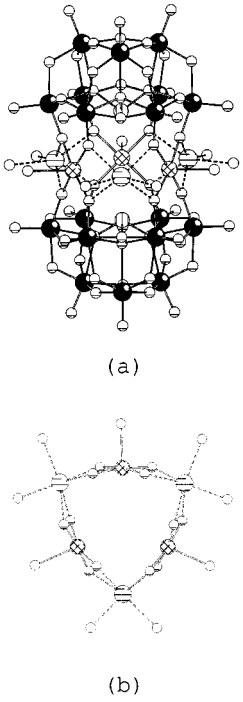

Figure 1. (a) Ball-and-stick diagram of $[Cu_3(H_2O)_3(\alpha\text{-}AsW_9O_{33})_2]^{12-}$ (**1**); this figure is also representative of $[Cu_3(H_2O)_3(\alpha\text{-}SbW_9O_{33})_2]^{12-}$ (**2**), $[Cu_3(H_2O)_3(\alpha\text{-}SeW_9O_{33})_2]^{10-}$ (**3**), and $[Cu_3(H_2O)_3(\alpha\text{-}TeW_9O_{33})_2]^{10-}$ (**4**); (b) representation of the central belt in **1**; Cu (cross-hatched), Na (horizontally hatched), As (vertically hatched), O (shaded), H_2O (unshaded)

Table 1. Cu···Cu and heteroatom (X···X) separations in polyanions **1**−**4**[26]

Polyanion	Cu···Cu [Å]	X···X [Å]
$[Cu_3(H_2O)_3(\alpha\text{-}AsW_9O_{33})_2]^{12-}$ (**1**)	4.69	5.34
$[Cu_3(H_2O)_3(\alpha\text{-}SbW_9O_{33})_2]^{12-}$ (**2**)	4.84	4.85
$[Cu_3(H_2O)_3(\alpha\text{-}SeW_9O_{33})_2]^{10-}$ (**3**)	4.84	5.38
$[Cu_3(H_2O)_3(\alpha\text{-}TeW_9O_{33})_2]^{10-}$ (**4**)	4.87	4.95

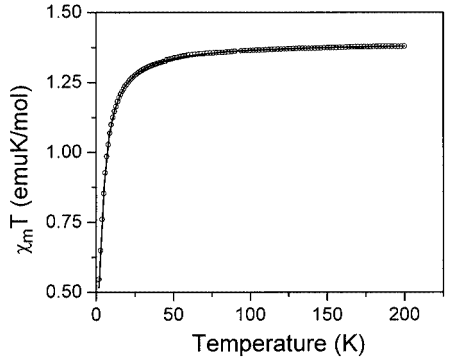

Figure 2. $\chi_m T$ vs. T plot of $K_9Na[Cu_3(H_2O)_3(\alpha\text{-}TeW_9O_{33})_2]\cdot 16H_2O$ (**K-4**) at H = 1000 G; the solid line represents the theoretical curve (see text)

Equation (2),[24,25,27] where S_T is the total spin and S_i (i = 1, 2, 3) is the spin of each ion.

$$\hat{H} = -2J[\hat{S}_1\cdot\hat{S}_2 + \hat{S}_2\cdot\hat{S}_3 + \hat{S}_3\cdot\hat{S}_1] \quad (1)$$

$$E(S_T,S_1,S_2,S_3) = -J[S_T(S_T+1) - S_1(S_1+1) - S_2(S_2+1) - S_3(S_3+1)] \quad (2)$$

Since for each Cu^{2+} ion $S_1 = S_2 = S_3 = 1/2$, S_T can take values 1/2 ($\uparrow\uparrow\downarrow$), 1/2 ($\uparrow\downarrow\uparrow$) or 3/2 ($\uparrow\uparrow\uparrow$). The S_T = 1/2 state is thus doubly degenerate, with an energy of $-3J/2$, while the S_T = 3/2 state has an energy of $3J/2$. Substitution of these values into the standard Van Vleck equation[28] yields the expression for the molar magnetic susceptibility [Equation (3)]. Here N is the Avogadro number, g the Landé g factor, β the electronic Bohr magneton, k the Boltzmann constant and T the temperature in Kelvin.

$$\chi_m = \frac{Ng^2\beta^2}{4kT}\left[\frac{1+5\exp(3J/kT)}{1+\exp(3J/kT)}\right] \quad (3)$$

The experimental $\chi_m T$ data for **Na-1**, **Na-2**, **K-3** and **K-4** have been fitted to Equation (3) by treating g and J as adjustable parameters. The agreement between the theoretical curve and the measured data is quite satisfactory. The best least-squares fit parameters are given in Table 2. The negative sign of J indicates the presence of antiferromagnetic intra-trimer interactions and hence, the doubly degenerate S_T = 1/2 state is the ground spin state in all four compounds. The g values are consistent with the g_{iso} values obtained directly from the EPR measurements (vide infra).

As indicated above, two of the three copper centers in **1**−**4** are crystallographically inequivalent, which inevitably results in two different Cu···Cu separations. Although these differences are very small (< 0.04 Å), we also attempted to fit the experimental data to an isosceles triangle model [cf. Equation (4)],[28] where J_1 and J_2 represent the two kinds of exchange interactions. Due to the similar magnetic environment, however, we could not improve the fits by using the two spin exchange constants J_1 and J_2.

$$\chi_m = \frac{Ng^2\beta^2}{4kT}\left[\frac{1+10\exp(3J_1/kT)+\exp(2(J_1-J_2)/kT)}{1+2\exp(3J_1/kT)+\exp(2(J_1-J_2)/kT)}\right] \quad (4)$$

In all four polyanions **1**−**4**, the Cu $3d_{x^2-y^2}$ orbitals, which contain the unpaired electrons, are directed along the $Cu-O_{eq}$ vectors. Therefore, spin exchange coupling takes place by an indirect pathway involving two tungsten and three oxygen atoms of each XW_9O_{33} (X = As^{III}, Sb^{III}, Se^{IV}, Te^{IV}) fragment. Hence, we expected weak spin exchange interactions between the Cu^{2+} ions. The small magnitude of the observed J values (ca. 1 cm^{-1}) supports this model (see Table 2).

The coupling constants J for **Na-1**, **Na-2**, **K-3** and **K-4** are plotted as a function of the Cu···Cu separations in Figure 3. It can be seen that for **Na-1**/**Na-2** and **K-3**/**K-4** there is a decrease of J with increasing Cu···Cu separation. The average equatorial $Cu-O_{eq}$ distances in polyanions **1**−**4** are very similar [**1**, 1.921(6) Å; **2**, 1.937(6) Å; **3**, 1.918(9) Å; **4**, 1.927(9) Å], so that the differences in the Cu···Cu separations between **1**−**4** must be due to the different heteroatoms. The heteroatoms of **1** (As^{III}) and **2** (Sb^{III}) are from main group V, whereas the hetero groups of **3** (Se^{IV}) and **4** (Te^{IV}) are from main group VI.

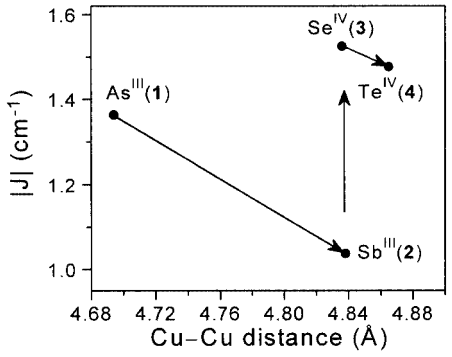

Figure 3. Dependence of the magnetic coupling constant J on the average Cu···Cu separations in $Na_{12}[Cu_3(H_2O)_3(\alpha\text{-}AsW_9O_{33})_2]\cdot 32H_2O$ (**Na-1**), $Na_{12}[Cu_3(H_2O)_3(\alpha\text{-}SbW_9O_{33})_2]\cdot 46H_2O$ (**Na-2**), $K_9Na[Cu_3(H_2O)_3(\alpha\text{-}SeW_9O_{33})_2]\cdot 16H_2O$ (**K-3**) and $K_9Na[Cu_3(H_2O)_3(\alpha\text{-}TeW_9O_{33})_2]\cdot 16H_2O$ (**K-4**)

When comparing **1** and **2**, it can be noted that both have the same charge, but the latter has the larger heteroatom. With the above in mind, the increase in the Cu···Cu separation in **2** compared to **1** must be due to an "equatorial expansion motion" of the former polyanion in the belt region. We believe that this is caused by lone pair···lone pair

Table 2. Magnetic parameters for polyanions **1**−**4** obtained from EPR and magnetic susceptibility measurements; the error in the g values is ± 0.005 and the error in J is ± 0.01

Polyanion	EPR							Susceptibility	
	S_T = 1/2			S_T = 3/2					
	$g_\parallel$	$g_\perp$	g_{iso}	$g_\parallel$	$g_\perp$	g_{iso}	D [cm^{-1}]	J [cm^{-1}]	g_{iso}
1 (X = As)[a]	2.117	2.254	2.208	2.060	2.243	2.182	0.0230	−1.36	2.209
2 (X = Sb)	2.128	2.257	2.219	2.061	2.231	2.175	0.0225	−1.04	2.223
3 (X = Se)	2.120	2.263	2.216	2.064	2.243	2.183	0.0219	−1.52	2.212
4 (X = Te)	2.127	2.288	2.234	2.065	2.239	2.181	0.0240	−1.48	2.226

[a] Ref.[8a]

interaction of the two heteroatoms, which is more pronounced in **2** than in **1** due to the larger size of Sb^{III} compared to As^{III} (see Table 1). The same trend is observed for **3** and **4** and we suggest an analogous explanation.

When comparing the magnetic exchange coupling constants *J* of **1** and **3** it must be remembered that the charge of the polyanions differs by 2 units. This is due to the fact that the heteroatoms are As^{III} and Se^{IV}, respectively. In **1** and **3** the heteroatom separation is essentially equivalent (see Table 1), so that the differences in the average Cu···Cu separation must be due to charge effects. The Cu···Cu separation is larger in **3** than in **1** which indicates an "equatorial expansion motion" similar to above, but this time it must be caused by excess negative charge on the polyanion. However, the exchange coupling constant *J* is larger for **3** than for **1**, indicating that an increase of the negative charge on the polyanion leads to an increase of the magnetic coupling constant. The same trend is observed for **2** and **4** and we suggest an analogous explanation. Nevertheless it remains to be seen if this observation can be generalized.

The two straight lines in Figure 3 perfectly reflect the size differences of the 4p (As^{III}, Se^{IV}) vs. 5p (Sb^{III}, Te^{IV}) heteroatoms. The fact that the slope of both lines is very similar indicates that the same trend is valid for group V and group VI heteroatoms. We have also shown that magnetic exchange coupling constants can reflect structural details of heteropolyanions. We believe that the graph in Figure 3 can also be used to predict coupling constants of related polyanions that have not yet been synthesized, e.g. the Bi derivative of **1** and **2**. We expect that the hypothetical polyanion $[Cu_3(H_2O)_3(\alpha\text{-}BiW_9O_{33})_2]^{12-}$ has a coupling constant *J* which is smaller than 1 cm^{-1}.

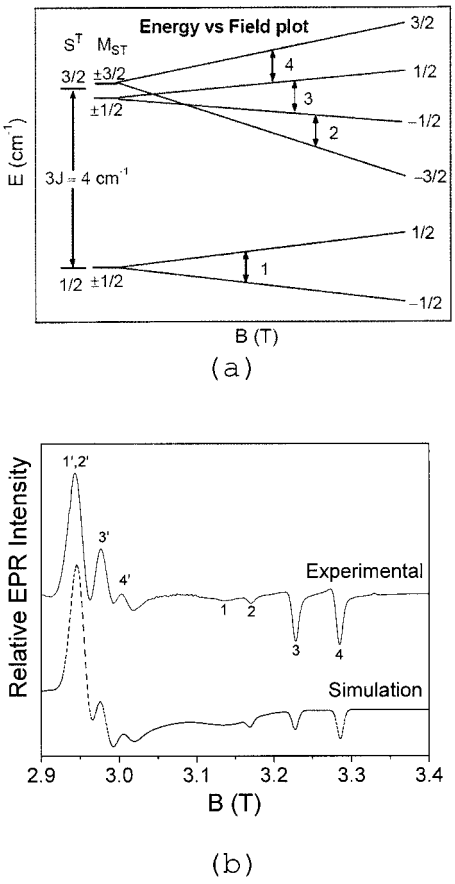

Figure 4. (a) Energy level diagram and the expected EPR transitions; (b) experimental and simulated W-band (ν = 93.494 GHz) powder EPR spectra of $K_9Na[Cu_3(H_2O)_3(\alpha\text{-}TeW_9O_{33})_2]\cdot 16H_2O$ (**K-4**) at 4 K

EPR Spectroscopy

Polycrystalline powder samples of **Na-1**, **Na-2**, **K-3** and **K-4** show similar EPR spectra with a quadruplet excited spin state at slightly higher energy than the S_T = 1/2 spin ground state (see Figure 4). The observed EPR spectra were analyzed using the spin Hamiltonian in Equation (5), where S_T is the total spin operator, *D* is the zero-field splitting parameter, and *g*, β, *B* have their usual meaning.

$$\hat{H} = \hat{S}_T \cdot D \cdot \hat{S}_T + \beta \cdot B \cdot g \cdot \hat{S}_T \quad (5)$$

The possible spin states correspond to a total spin of S_T = 3/2 or 1/2, which is expected for a frustrated triangle containing an unpaired electron et each vertex. Here we neglect the hyperfine structure due to the $^{63,65}Cu$ nuclei, since it is exchange-averaged. Also, we do not consider *J* here because its effect is not detected by standard EPR measurements, except through the detection of separate spectra from the ground and thermally accessible excited states. The small magnitude of exchange determined by magnetic susceptibility is not large enough to see intensity changes between different spin states.[25] Assuming axial symmetry, and the high-field limit ($g\beta B >> |D|$, as is the case here), the solution of Equation (5) is straightforward.[29] The line centers will be given by the *g* factor, and each line will be split into $2S_T$ components. For a system with axial symmetry, such as the $(Cu^{2+})_3$ moiety here, the fine structure splitting varies essentially as $D(3\cos^2\Theta - 1)$, where Θ is the angle between the applied field direction and the axis of symmetry. Thus, for an S_T = 3/2 spin state, the powder pattern in the limit $g\beta B >> |D|$ should consist of a triplet around the principal *g* components. The triplet separation around the *g* peak is 2*D* while the separation of perpendicular transitions around the $g_{\|}$ peak is 2|*D*|.

Figure 4 (a) shows the energy level diagram and the expected magnetic dipole ($\Delta M_{ST} = \pm 1$) transitions, labeled 1−4. Figure 4 (b) shows the 4 K experimental W-band EPR spectrum of the tellurium analog **K-4** with the best-fit simulation. The experimental spin Hamiltonian parameters used in this simulation and those obtained for compounds **Na-1**, **Na-2** and **K-3** are summarized in Table 2. Figure 5 shows the measured room-temperature and 4 K W-band EPR spectra for **K-4**. In the room-temperature spectrum, only the quadruplet fine structure transitions are observed for the quadruplet excited spin state. At 4 K, a fourth parallel peak centered at *g* = 2.117 was observed. The higher intensity of the lowest field line suggests that the perpendicular component of the S_T = 1/2 state is superimposed. This ob-

servation lends credence to a lower energy spin state being present. The ground spin state for the $(Cu^{2+})_3$ triangle is therefore the doublet $S_T = 1/2$ state. Further analysis of the signal intensity with respect to temperature reveals the sign of the zero field splitting. At lowest temperature, only the lowest energy states are thermally populated. Hence, at 4 K, the fine structure line intensity shifts into the outermost parallel and perpendicular lines, indicating a positive sign for the D value. The $M_{ST} = \pm 1/2$ states are therefore of lower energy. Compounds **Na-1**, **Na-2**, **K-3** have analogous EPR spectra and show an $S_T = 1/2$ ground spin state; however, the magnetic parameters vary slightly. It should be noted that in all cases the quadruplet state transitions are still observed at 4 K because the spin exchange between states is small (ca. 4 cm^{-1}).

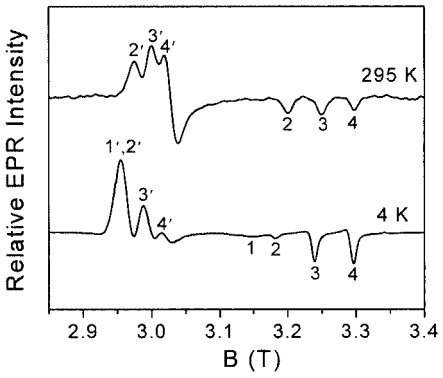

Figure 5. W-band (ν = 93.494 GHz) powder EPR spectra of $K_9Na[Cu_3(H_2O)_3(\alpha\text{-}TeW_9O_{33})_2]\cdot 16H_2O$ (**K-4**) at 295 K and 4 K as indicated; numbering corresponds to Figure 4 (a)

The geometrical arrangement of the CuO_5 groups in polyanions **1**−**4** is such that their perpendicular directions correspond to the C_3 axis of the heteropolyanion, while the parallel direction of each CuO_5 unit is perpendicular to the molecular C_3 axis. The square-pyramidal geometry of each CuO_5 unit has C_{4v} site symmetry. Since, the axial Cu−Ow distance in each unit is longer than the four equatorial Cu−O distances,[26] the $3d_{z^2}$ orbital is stabilized with respect to $3d_{x^2-y^2}$ such that the unpaired electron resides in the $3d_{x^2-y^2}$ orbital. Siedle et al. have shown that the observed EPR g matrix parameters can be transformed with respect to the g matrix of the individual copper centers.[30] If g(m) represents the g matrix of an individual CuO_5 unit, the relation between g(m) and the observed g values can be written as $g_{\|} = g_{\perp}(m)$ and $g_{\perp} = (1/2)[g_{\|}(m) + g_{\perp}(m)]$. Applying these relations to the polyanion **4**, for example, yields $g_{\|}(m)$ and $g_{\perp}(m)$ values as 2.449 and 2.127, respectively. With this geometrical framework $g_{\|}(m) > g_{\perp}(m) > g_e$, g_e being the free electron g value of 2.0023, proving that the $d_{x^2-y^2}$ orbital contains the unpaired electron.

Finally, an interesting observation from Table 2 is that for **4**, the D value magnitude does not fit the trend of the Cu···Cu distances. Normally, one would expect that the D value should fall off sensitively with the Cu···Cu separations. For **4**, however, while the Cu···Cu distance is the largest, the D value is also the largest. This breakdown in the D value vs. Cu···Cu distance relationship suggests a significant role for the through-bond interactions in **4**.

Conclusions

W-band EPR and SQUID measurements have enabled us to measure the influence of the charge and size properties of the lone pair containing heteroatoms on the central Cu^{2+} triangle embedded in a series of four isostructural polyoxometalates. The g_{iso} value calculated from EPR measurements for the ground spin state for compounds **Na-1**, **Na-2**, **K-3** and **K-4** varies from the best fit parameters determined by $\chi_m T$ vs. T plots. For **Na-1** and **K-3**, which have larger J values, the agreement between magnetic susceptibility and EPR spectroscopic results is within experimental error. For **Na-2** and **K-4**, a 3% difference was observed in the g values determined from the two techniques. We tentatively ascribe this difference to the fact that the susceptibility measurements extend over a wide temperature range.

In summary, we have performed the first systematic study of the magnetic properties of an isostructural family of polyoxoanions. Not surprisingly, magnetic susceptibility and EPR measurements have revealed that the magnetic exchange coupling constant J is a sensitive parameter that can reflect very small structural differences in the magnetic core (e.g. Cu···Cu separations) of polyanions. More importantly, we have also shown that these structural differences can be rationalized by size and charge effects of the heteroatoms. This means that magnetic measurements can be used as an indirect analytical tool, in order to investigate phenomena that originate in nonmagnetic regions of magnetic molecules.

Experimental Section

Synthesis: The polyoxoanions $Na_{12}[Cu_3(H_2O)_3(\alpha\text{-}AsW_9O_{33})_2]\cdot 32H_2O$ (**Na-1**), $Na_{12}[Cu_3(H_2O)_3(\alpha\text{-}SbW_9O_{33})_2]\cdot 46H_2O$ (**Na-2**), $K_9Na[Cu_3(H_2O)_3(\alpha\text{-}SeW_9O_{33})_2]\cdot 16H_2O$ (**K-3**) and $K_9Na[Cu_3(H_2O)_3(\alpha\text{-}TeW_9O_{33})_2]\cdot 16H_2O$ (**K-4**) were synthesized according to the published procedure.[26]

Magnetic Susceptibility Measurements: Magnetic susceptibility measurements on **Na-1**, **Na-2**, **K-3** and **K-4** were carried out using a Quantum Design MPMS-XL SQUID magnetometer. Data for polycrystalline samples were collected over 1.8−200 K at 1000 G, using approximately 70 mg of sample. The data were corrected for the sample holder, diamagnetism using Klemm constants,[31] and temperature-independent paramagnetism (TIP) contributions.

EPR Spectroscopy: Polycrystalline powder EPR spectra of **Na-1**, **Na-2**, **K-3** and **K-4** were recorded at W-band frequencies (ca. 94 GHz) at the high-field electron magnetic resonance facility at the National High Magnetic Field Laboratory in Tallahassee, as described elsewhere.[32,33] Temperature variation was measured from room temperature to 4 K. An Oxford Instruments Teslatron superconducting magnet, able to sweep between 0 and 17 T, was used to apply the Zeeman field. In all experiments the modulation

amplitudes and microwave power were adjusted for optimal signal intensity and resolution. The Bruker XSophe EPR simulation program was used with the appropriate spin Hamiltonian to generate simulated EPR spectra. This program includes a Boltzmann term that considers thermal population of particular spin levels.

Acknowledgments

The work at NHMFL was supported in part by the NSF and the State of Florida. We wish to thank Dr. Johan van Tol for his helpful advice and discussions. U. K. thanks the International University Bremen for research support. Figure 1 was generated by Diamond Version 2.1e (© Crystal Impact GbR).

[1] M. T. Pope, *Heteropoly and Isopoly Oxometalates*, Springer, Berlin, **1983**.
[2] M. T. Pope, A. Müller, *Angew. Chem.* **1991**, *103*, 56−70; *Angew. Chem. Int. Ed. Engl.* **1991**, *30*, 34−48.
[3] *Polyoxometalates: from Platonic Solids to Anti Retroviral Activity* (Eds.: M. T. Pope, A. Müller), Kluwer, Dordrecht, **1994**.
[4] Special Thematic Issue on Polyoxometalates: *Chem. Rev.* **1998**, *98*, 1−389.
[5] *Polyoxometalate Chemistry: From Topology via Self-Assembly to Applications* (Eds.: M. T. Pope, A. Müller), Kluwer, Dordrecht, **2001**.
[6] *Polyoxometalate Chemistry for Nano-Composite Design* (Eds.: T. Yamase, M. T. Pope), Kluwer, Dordrecht, **2002**.
[7] [7a] For a recent review on the potential of high-spin systems for nanotechnology, see: J. Tejada, E. M. Chudnovsky, E. del Barco, J. M. Hernandez, *Nanotechnology* **2001**, *12*, 181−186. [7b] For their importance in fundamental research, see: D. Gatteschi, R. Sessoli, *Angew. Chem. Int. Ed.* **2003**, *42*, 268−297. [7c] For quantum computation, see: D. Loss, M. Leuenberger, *Nature (London)* **2000**, *410*, 789−793. [7d] For some general references, see: J. R. Friedman, M. P. Sarachik, J. Tejada, R. Ziolo, *Phys. Rev. Lett.* **1996**, *76*, 3830−3833; C. Sangregorio, T. Ohm, C. Paulsen, R. Sessoli, D. Gatteschi, *Phys. Rev. Lett.* **1997**, *78*, 4645−4648; A. L. Barra, D. Gatteschi, R. Sessoli, *Phys. Rev. B* **1997**, *56*, 8192−8198; J. A. A. J. Perenboom, J. S. Brooks, S. Hill, T. Hathaway, N. S. Dalal, *Phys. Rev. B* **1998**, *58*, 330−338; S. Hill, J. A. A. J. Perenboom, N. S. Dalal, T. Hathaway, T. Stalcup, J. S. Brooks, *Phys. Rev. Lett.* **1998**, *80*, 2453−2456; L. Bokacheva, A. D. Kent, M. A. Walters, *Phys. Rev. Lett.* **2000**, *85*, 4803−4806; E. M. Chudnovsky, D. A. Garanin, *Phys. Rev. B* **2002**, *65*, 094423−094431 and references cited therein for theoretical work.
[8] [8a] U. Kortz, S. Nellutla, A. C. Stowe, N. S. Dalal, J. van Tol, B. Bassil, *Inorg. Chem.* **2004**, *43*, 144−154. [8b] U. Kortz, S. Nellutla, A. C. Stowe, N. S. Dalal, U. Rauwald, W. Danquah, D. Ravot, *Inorg. Chem.* **2004**, *43*, 2308−2317, and references cited therein.
[9] R. Sessoli, D. Gatteschi, A. Caneschi, M. A. Novak, *Nature* **1993**, *365*, 141−143.
[10] O. Kahn, *Chem. Phys. Lett.* **1997**, *265*, 109−114.
[11] G. Aromí, S. M. J. Aubin, M. A. Bolcar, G. Christou, H. J. Eppley, K. Folting, D. N. Hendrickson, J. C. Huffman, R. C. Squire, H.- L. Tsai, S. Wang, M. W. Wemple, *Polyhedron* **1998**, *17*, 3005−3020.
[12] For detailed references, see: [12a] S. M. J. Aubin, Z. Sun, H. J. Eppley, E. M. Rumberger, E. A. Guzei, K. Folting, P. K. Gantzel, A. L. Rheingold, G. Christou, D. N. Hendrickson, *Inorg. Chem.* **2001**, *40*, 2127−2146. [12b] D. Gatteschi, R. Sessoli, *Angew. Chem.* **2003**, *115*, 278−309. [12c] G. Christou, D. Gatteschi, D. N. Hendrickson, R. Sessoli, *MRS Bull.* **2000**, *25*, 66−71.
[13] G. F. Kokoszka, F. Padula, A. S. Goldstein, E. L. Venturini, L. Azevedo, A. R. Siedle, *Inorg. Chem.* **1988**, *27*, 59−62.
[14] [14a] L. C. W. Baker, V. E. S. Baker, S. H. Wasfi, G. A. Candela, A. H. Kahn, *J. Am. Chem. Soc.* **1972**, *94*, 5499−5501. [14b] L. C. W. Baker, V. E. S. Baker, S. H. Wasfi, G. A. Candela, A. H. Kahn, *J. Chem. Phys.* **1972**, *56*, 4917−4923.
[15] Some recent references include: [15a] U. Kortz, S. Isber, M. H. Dickman, D. Ravot, *Inorg. Chem.* **2000**, *39*, 2915−2922. [15b] L.-H. Bi, R.-D. Huang, J. Peng, E.-B. Wang, Y.-H. Wang, C.-W. Hu, *J. Chem. Soc., Dalton Trans.* **2001**, 121−129. [15c] E. M. Limanski, M. Piepenbrink, E. Droste, K. Burgemeister, B. Krebs, *J. Cluster Sci.* **2002**, *13*, 369−379.
[16] [16a] C. J. Gómez-García, E. Coronado, J. J. Borrás-Almenar, *Inorg. Chem.* **1992**, *31*, 1667−1673. [16b] N. Casañ-Pastor, J. Bas-Serra, E. Coronado, G. Pourroy, L. C. W. Baker, *J. Am. Chem. Soc.* **1992**, *114*, 10380−10383. [16c] C. J. Gómez-García, E. Coronado, P. Gómez-Romero, N. Casañ-Pastor, *Inorg. Chem.* **1993**, *32*, 3378−3381. [16d] C. J. Gómez-García, J. J. Borrás-Almenar, E. Coronado, L. Ouahab, *Inorg. Chem.* **1994**, *33*, 4016−4022. [16e] J. M. Clemente-Juan, E. Coronado, J. R. Galán-Mascarós, C. J. Gómez-García, *Inorg. Chem.* **1999**, *38*, 55−63.
[17] E. Sinn, *Coord. Chem. Rev.* **1970**, *5*, 313−347.
[18] J. S. Griffith, *Struct. Bonding (Berlin)* **1972**, *10*, 87.
[19] B. S. Tsukerblat, V. M. Novotortsev, B. Y. Kuyavskaya, M. I. Belinsky, A. V. Ablov, A. N. Bazhan, V. T. Kalinnikov, *Sov. Phys. JETP Lett.* **1974**, *19*, 277−278.
[20] [20a] L. Banci, A. Bencini, D. Gatteschi, *Inorg. Chem.* **1983**, *22*, 2681−2683. [20b] L. Banci, A. Bencini, A. Dei, D. Gatteschi, *Inorg. Chem.* **1983**, *22*, 4018−4021.
[21] J. Padilla, D. Gatteschi, P. Chaudhuri, *Inorg. Chim. Acta* **1997**, *260*, 217−220.
[22] M. Azuma, T. Odaka, M. Takano, D. A. Vander Griend, K. R. Poeppelmeier, Y. Narumi, K. Kindo, Y. Mizuno, S. Maekawa, *Phys. Rev. B* **2000**, *62*, R3588−R3591.
[23] M. Kodera, Y. Tachi, T. Kita, H. Kobushi, Y. Sumi, K. Kano, M. Shiro, M. Koikawa, T. Tokii, M. Ohba, H. Okawa, *Inorg. Chem.* **2000**, *39*, 226−234.
[24] R. Clérac, F. A. Cotton, K. R. Dunbar, E. A. Hillard, M. A. Petrukhina, B. W. Smuckler, *C. R. Acad. Sci. Ser. IIc: Chim.* **2001**, *4*, 315−319.
[25] B. Cage, F. A. Cotton, N. S. Dalal, E. A. Hillard, B. Rakvin, C. M. Ramsey, *J. Am. Chem. Soc.* **2003**, *125*, 5270−5271; *C. R. Chim.* **2003**, *6*, 39−46.
[26] U. Kortz, N. K. Al-Kassem, M. G. Savelieff, N. A. Al Kadi, M. Sadakane, *Inorg. Chem.* **2001**, *40*, 4742−4749.
[27] K. Kambe, *J. Phys. Soc., Jpn.* **1950**, *5*, 48−51.
[28] O. Kahn, *Molecular Magnetism*, VCH, New York, **1993**.
[29] A. Abragam, B. Bleaney, *Electron Paramagnetic Resonance of Transition Ions*, Dover Publications, Inc., New York, **1970**.
[30] A. R. Siedle, F. Padula, J. Baranowski, C. Goldstein, M. DeAngelo, G. F. Kokoszka, L. Azevedo, E. L. Venturini, *J. Am. Chem. Soc.* **1983**, *105*, 7447−7448.
[31] S. G. Vulfson, *Molecular Magnetochemistry*, Gordon and Breach Science, The Netherlands, **1998**, p. 241.
[32] B. Cage, A. K. Hassan, L. Pardi, J. Krzystek, L.-C. Brunel, N. S. Dalal, *J. Magn. Reson.* **1997**, *124*, 495−498.
[33] A. K. Hassan, L. A. Pardi, J. Krzystek, A. Sienkiewicz, P. Goy, M. Rohrer, L.-C. Brunel, *J. Magn. Reson.* **2000**, *142*, 300−312.

Received March 23, 2004
Early View Article
Published Online July 29, 2004

